Progress In Electromagnetics Research C, Vol. 165, 221–227, 2026

PIER C

(Received 17 December 2025, Accepted 16 January 2026, Scheduled 1 February 2026)

Propagation of Electromagnetic Wave in 1D Perfect Periodic Parallel Waveguides and Resonators Using Transfer Matrix Method

Moulay S. Khattab, Tarik Touiss*, and Driss Bria

Laboratory of Materials, Waves, Energy and Environment
Team of Waves, Acoustics, Photonics and Materials, Mohamed I University, Oujda, Morocco

ABSTRACT: The results of the propagation of electromagnetic waves in 1D periodic photonic waveguides and resonators are presented in this study. This structure consists of periodically arranged cells, with each cell containing parallel and series segments, grafted by two resonators at two different sites. This system creates passbands separated by photonic bandgaps, in which electromagnetic waves cannot propagate. The analytical calculation is based on the transfer matrix method (TMM), which aims to calculate the dispersion relation and transmission rate. Our results indicate the importance of the resonator length in applications, such as guiding and filtering electromagnetic waves. This study also demonstrates how the addition of cells and the adjustment of resonator lengths influence the frequency selectivity, which is essential for filtering in communication technologies.

1. INTRODUCTION

The study of electromagnetic wave propagation in periodic waveguide structures has been a focus of interest in recent decades, leading to significant advances in various fields of research [1–3]. These structures are characterized by a central waveguide with multiple lateral branches or resonators at each site, which offer unique electromagnetic properties. This distinctive design plays an essential role, particularly in electromagnetic technology and photonics [4, 5]. One of the main features of these structures is the presence of photonic band gaps (PBGs) [6], which are separated by narrow passbands. The strategic positioning and dimensions of these band gaps are crucial for the development of devices designed to reflect or confine electromagnetic waves [7]. This study focuses on the relationship between the structural design of periodic waveguides and their electromagnetic properties, underlining the importance of PBGs in current electromagnetic and photonic applications [8, 9].

Concerning specific contributions to periodic systems, Antraoui and Khettabi [10] examined the propagation of acoustic waves in a 1D comb-like periodic structure in the presence of a defective open resonator situated in the middle of the perfect periodic structure using the transfer matrix method (TMM) and Sylvester's theorem. El Kadmiri et al. [11] showed that there is a double frequency filtering based on two defect modes in an enormous gap by creating a defect at the segment and opening resonator levels in a one-dimensional comb-like phononic structure. On the other hand, Ben Ali et al. [12] studied new filters based on the defect modes by using defective resonators in this structure containing left-handed materials. In addition, Vasseur et al. [13] demonstrated the presence of defect modes in the band gaps by integrating defective branches of different lengths and materials into star waveguide structures. Finally, the existence of band gaps was experimentally demonstrated by Dobrzyński et al. [14] who used coaxial cables in the frequency range up to 500 MHz.

The present research is based on a recent study presented in [15], which studied electromagnetically induced transparency (EIT) and Fano resonances in one cell in order to develop multichannel electromagnetic filters. The present study extends this previous study by considering the propagation of electromagnetic waves in finite and infinite periodic systems composed of parallel waveguides coupled to asymmetric resonators. In contrast to [15], where the analysis was limited to an isolated or finite structure, the introduction of periodicity in the present study allows the derivation of Bloch dispersion relation and the identification of photonic bandgaps and passbands. Furthermore, this study systematically examines the influence of geometrical parameters and the number of unit cells on wave propagation and frequency selectivity, highlighting the crucial role of resonator lengths in controlling the position and width of photonic band gaps, thereby enabling more advanced and highly selective electromagnetic filtering.

The propagation of electromagnetic waves through the photonic structure was theoretically investigated in this work (Figure 1). This article is organized as follows. A detailed analytical calculation of the dispersion relation, transmission and reflection rates using the TMM is presented in Section 2. The

* Corresponding author: Tarik Touiss (tariktouiss22@gmail.com).

doi:10.2528/PIERC25121701

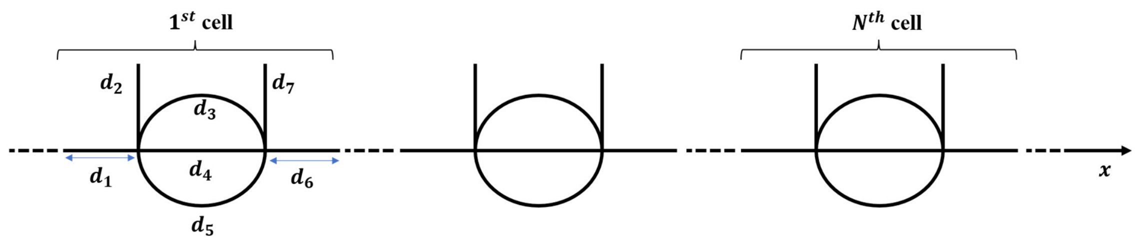

FIGURE 1. Geometrical representation of the periodic structure. The system can be physically implemented using coaxial cables. Each unit cell consists of longitudinal series waveguide segments (d_1, d_6), three parallel branches (d_3, d_4, d_5), and two lateral resonators of lengths d_2 and d_7 grafted at different positions.

numerical results and discussion are presented in Section 3. In Section 4, we present the main summary of this study.

For clarity, the physical meaning of the geometrical parameters defining the unit cell in Figure 1 is specified as follows. The proposed structure can be physically realized using coaxial cables, as commonly employed in experimental investigations of one-dimensional electromagnetic waveguides [16]. In this context, all segments of lengths d_1 to d_7 correspond to coaxial cable sections with identical characteristic impedance and dielectric properties. The lengths d_1 and d_6 represent the main longitudinal coaxial waveguide sections connected in series, ensuring electromagnetic wave propagation along the structure. The segments d_3, d_4, and d_5 correspond to parallel coaxial branches that introduce multiple propagation paths and coupling effects. The parameters d_2 and d_7 denote the lengths of two lateral coaxial resonators grafted at different positions within the unit cell. These resonators are responsible for local resonant phenomena, such as Fano or electromagnetically induced transparency (EIT)-like resonances, and play a key role in the formation and tuning of photonic band gaps.

2. MODEL AND FORMALISM

Our theoretical analysis is based on the formalism of the transfer matrix method, and we calculate the dispersion relation and transmission and reflection rates. The expressions for the electric fields in the segment and resonator are given by [15, 17–19]:

$$E(x,y)=\begin{cases} E_0\left(x\right)=A_0e^{j\alpha_0 x}+B_0e^{-j\alpha_0 x} & \text{for: } x\le 0 \\ E_1\left(x\right)=A_1e^{j\alpha_1 x}+B_1e^{-j\alpha_1 x} & \text{for: } 0\le x\le d_1 \\ E_2\left(y\right)=C_0e^{j\alpha_2 y}+D_0e^{-j\alpha_2 y} & \text{for: } 0\le y\le d_2 \\ E_s\left(x\right)=A_se^{j\alpha_s(x-d_1)} & \text{for: } x\ge d_1 \end{cases} \tag{1}$$

The electric field distribution within each medium is expressed as the sum of the incident and reflected waves. α_i is the wave number in medium "i" ($i=0,1,2,s$), and the coefficients A_n and B_n are constants ($n=0,1,s$).

We use the conditions of the passage of electric fields and find the transfer matrix of segment length d_1 and grafted resonator length d_2 in the following form [15, 17]:

$$M_1=\begin{pmatrix} C_1-\frac{\alpha_2 S_2}{\alpha_1 C_2}S_1 & -j\frac{S_1}{\alpha_1} \\ -j\alpha_1 S_1-j\frac{\alpha_2 S_2}{C_2}C_1 & C_1 \end{pmatrix} \tag{2}$$

with:

$$C_i=\text{Cos}(\alpha_i d_i),\quad S_i=\text{Sin}(\alpha_i d_i)$$

$$\text{and}\quad \alpha_i=\frac{\omega}{c}\sqrt{\mu_i\varepsilon_i}\quad (i=1,2) \tag{3}$$

The transfer matrix of a single segment is:

$$\begin{pmatrix} A_0 \\ B_0 \end{pmatrix}=M_i\begin{pmatrix} A_S \\ B_S \end{pmatrix}=\begin{pmatrix} C_i & -j\frac{S_i}{\alpha_i} \\ -j\alpha_i S_i & C_i \end{pmatrix}\begin{pmatrix} A_S \\ B_S \end{pmatrix}$$

$$=\begin{pmatrix} T_{i,11} & T_{i,12} \\ T_{i,21} & T_{i,22} \end{pmatrix}\begin{pmatrix} A_S \\ B_S \end{pmatrix} \tag{4}$$

We use the admittance matrix to calculate the transfer matrix of the three parallel segments. The segment admittance matrix is:

$$\begin{pmatrix} B_0 \\ B_s \end{pmatrix}=Y_i\begin{pmatrix} A_0 \\ A_S \end{pmatrix}=\begin{pmatrix} y_{i,11} & y_{i,12} \\ y_{i,21} & y_{i,22} \end{pmatrix}\begin{pmatrix} A_0 \\ A_S \end{pmatrix} \tag{5}$$

We use the admittance matrix to calculate the transfer matrix of three parallel segments of lengths d_3, d_4, and d_5:

$$\begin{pmatrix} B_0 \\ B_s \end{pmatrix}=Y_T\begin{pmatrix} A_0 \\ A_S \end{pmatrix}=\sum\nolimits_{i=1}^{3}Y_i\begin{pmatrix} A_0 \\ A_S \end{pmatrix}$$

$$=\begin{pmatrix} \sum_{i=1}^{3}y_{i,11} & \sum_{i=1}^{3}y_{i,12} \\ \sum_{i=1}^{3}y_{i,21} & \sum_{i=1}^{3}y_{i,22} \end{pmatrix}\begin{pmatrix} A_0 \\ A_S \end{pmatrix} \tag{6}$$

The transfer matrix of three parallel segments is given by [15]:

$$\begin{pmatrix} A_0 \\ B_0 \end{pmatrix}=M_2\begin{pmatrix} A_S \\ B_S \end{pmatrix}=\frac{-1}{\sum_{i=1}^{3}y_{i,21}}\begin{pmatrix} \sum_{i=1}^{3}y_{i,22} & -1 \\ \sum_{i=1}^{3}y_{i,22}\cdot\sum_{i=1}^{3}y_{i,11}-\sum_{i=1}^{3}y_{i,12}\cdot\sum_{i=1}^{3}y_{i,21} & -\sum_{i=1}^{3}y_{i,11} \end{pmatrix}\begin{pmatrix} A_S \\ B_S \end{pmatrix} \tag{7}$$

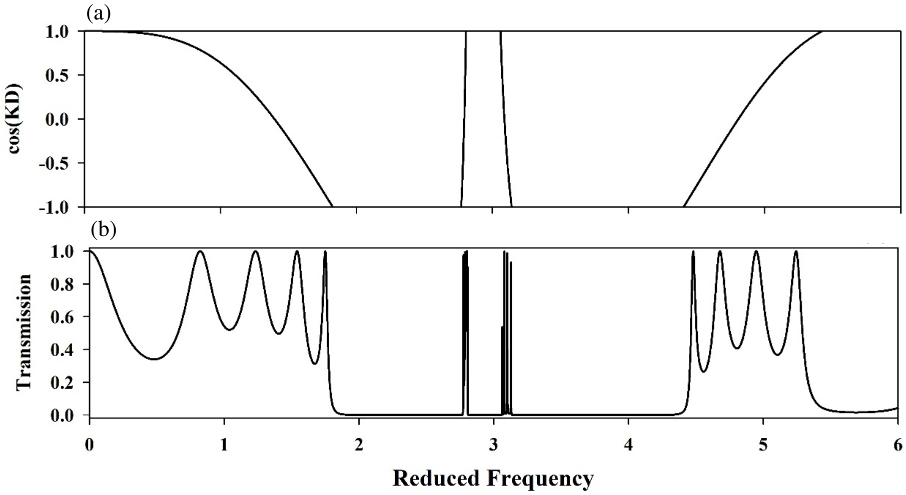

FIGURE 2. (a) Spectrum of the dispersion relation. (b) Spectrum of the transmission rate as a function of the reduced frequency of the perfect periodic structure with $N = 5$, $d_1 = 0.5D$, $d_2 = d_7 = 0.54D$, $d_3 = d_4 = d_5 = 1D$ and $d_6 = 1.5D$.

The transfer matrix of segment length d_6 and grafted resonator length d_7 is:

$$M_3 = \begin{pmatrix} C_6 & -j\frac{S_6}{\alpha_6} \\ -j\alpha_6 S_6 - j\frac{\alpha_7 S_7}{C_7} C_6 & C_6 - \frac{\alpha_7 S_7}{\alpha_6 C_7} S_6 \end{pmatrix} \quad (8)$$

The transfer matrix of a cell is given by:

$$M_{cell_1} = M_1 \cdot M_2 \cdot M_3 = \begin{pmatrix} T_{11} & T_{12} \\ T_{21} & T_{22} \end{pmatrix} \quad (9)$$

The dispersion relation of the infinite system is given by:

$$\cos(KD) = \frac{\text{tr}(M_{cell_1})}{2} \quad (10)$$

where K represents the Bloch vector.

The considered system is composed of N cells (Figure 1), and the matrix corresponding to this periodic structure can be obtained by calculating the product of each matrix as follows:

$$M_T = \prod_{i=1}^{N} M_{cell_i} = \begin{pmatrix} T_{11} & T_{12} \\ T_{21} & T_{22} \end{pmatrix}^N \quad (11)$$

The unit matrix of order N can be simplified by the following identity matrix:

$$\begin{pmatrix} T_{11} & T_{12} \\ T_{21} & T_{22} \end{pmatrix}^N = \begin{pmatrix} T_{11}U_N - U_{N-1} & T_{12}U_N \\ T_{21}U_n & T_{22}U_N - U_{N-1} \end{pmatrix} \quad (12)$$

where $U_N = \frac{\sin(NKD)}{\sin(KD)}$, the reflection and transmission rates of the perfect structure are given by:

$$\begin{cases} T_N = \\ \left| \frac{2}{\left[T_{11}U_N - U_{N-1} + \alpha_s T_{12} U_N + \frac{T_{21}U_n}{\alpha_0} + (T_{22}U_N - U_{N-1})\left(\frac{\alpha_s}{\alpha_0}\right)\right]} \right|^2 \\ R_N = \\ \left| \frac{\left[T_{11}U_N - U_{N-1} + \alpha_s T_{12} U_N - \frac{T_{21}U_n}{\alpha_0} - (T_{22}U_N - U_{N-1})\left(\frac{\alpha_s}{\alpha_0}\right)\right]}{\left[T_{11}U_N - U_{N-1} + \alpha_s T_{12} U_N + \frac{T_{21}U_n}{\alpha_0} + (T_{22}U_N - U_{N-1})\left(\frac{\alpha_s}{\alpha_0}\right)\right]} \right|^2 \end{cases} \quad (13)$$

3. RESULTS AND DISCUSSIONS

In this section, we numerically illustrate the propagation of electromagnetic waves through a periodic system in which each cell contains parallel segments and symmetrical/asymmetrical resonators (Figure 1). We take the dielectric permittivity of the segments and resonators as $\varepsilon_i = 2.3$ (polyethylene), and the magnetic permeability of the materials is $\mu_i = 1$ (non-magnetic medium), where 'i' indicates the medium $(i = [1 - 7])$. The reduced frequency is given by $\Omega = \frac{\omega D\sqrt{\varepsilon_i \mu_i}}{c}$ which is a dimensionless quantity; D is a unit of length; c is the velocity of electromagnetic waves in vacuum; and ω is the pulsation. It should be noted that the reduced frequency Ω and all geometric parameters used in this work are normalized quantities and therefore dimensionless. This normalization allows for general and scalable results, without reference to a specific physical length or frequency scale.

3.1. Analysis of Dispersion and Transmission Spectra in the Perfect Periodic Structure

Figure 2 shows two related physical concepts found in the study of wave dynamics within periodic structures, such as photonic crystals, acoustic waveguides or photonic waveguides. Figure 2(a) illustrates the spectrum of the dispersion relation in

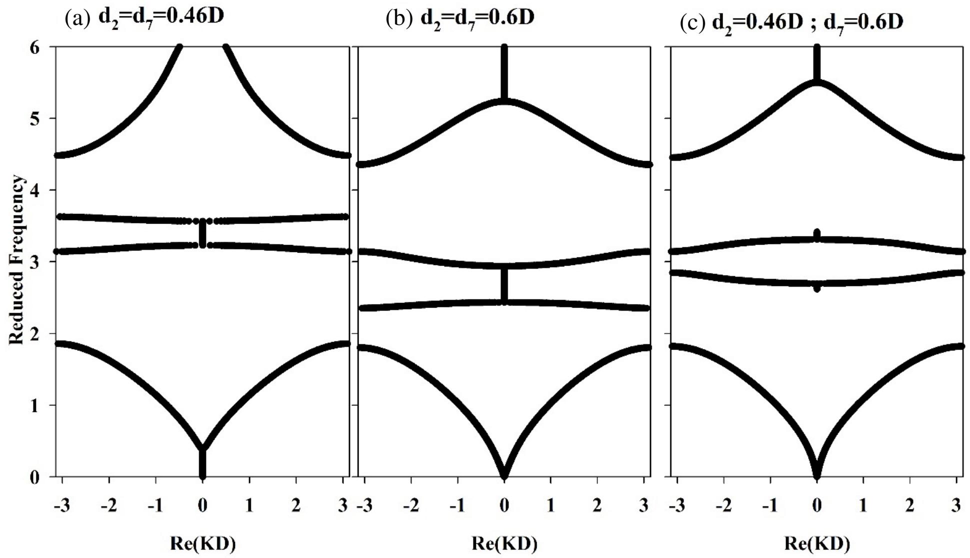

FIGURE 3. Variation of the reduced frequency Ω as a function of the real part of KD of the infinite periodic system for different values of d_2 and d_7, with $d_1 = 0.5D$, $d_3 = d_4 = d_5 = 1D$ and $d_6 = 1.5D$.

a periodic system, showing the real part of the Bloch vector (K) (is a representation of the periodicity of the structure in the wave-vector space) and a characteristic dimension (D). This representation clearly shows that the system allows for specific frequencies where the phase effects of a wave repeatedly pass through a period of the structure. This reveals the band structure of the material, where the value of $\cos(KD)$ varies between -1 and $+1$, indicating the passband (allowing waves to propagate). Figure 2(b) shows the transmission spectrum for a finite periodic system, where the transmission peaks indicate the passband frequencies where the propagation of electromagnetic waves is permitted, whereas the band gaps indicate that the electromagnetic waves cannot propagate. The two cases show a clear correspondence between the passbands and $\cos(KD)$ values in the allowed region. The presence of band gaps and band pass is crucial for technological applications, particularly in the design of optical filters and waveguides, where control of the propagation wave is necessary. In practice, the ability to precisely control transmission frequencies through structural design is important for the development of telecommunications and optical filtering devices.

3.2. Variation of the Reduced Frequency as a Function of Real Part of the Bloch Vector

Figure 3 presents the band structure of an infinite periodic system, showing the variation in the reduced frequency with the real part of the Bloch vector. Figures 3(a), (b), and (c) correspond to different cases, with parameters d_2 and d_7 taking the values of $0.46D$ and $0.6D$ in various combinations. These graphs are essential for determining the transport properties of waves, such as optics for photons or acoustics for phonons [20]. The real part of the wave vector is related to the phase velocity of the wave and periodicity of the medium, whereas the imaginary part of the KD wave vector is typically associated with the attenuation of the wave inside the band gaps. Passbands are areas where the real part of KD corresponds to propagation modes. The black branches (solid black lines) represent the passbands, where electromagnetic waves can propagate through the structure with minimal attenuation. It can be observed that the change in d_2 from $0.46D$ to $0.6D$ between plots (a) and (b) changes the position and width of the band gaps, which could affect the behaviour of the waves as they interact with the material. Similarly, the combination of the two values in (c) produces a combined effect on the band structure, showing the importance of the interaction between different lengths in the material. In all the cases, the absence of features was due to destructive interference.

3.3. Effects of Cell Number

Figure 4 shows the transmission rate as a function of the reduced frequency for different numbers of cells, N, with $d_1 = 0.5D$, $d_2 = d_7 = 0.54D$, $d_3 = d_4 = d_5 = 1D$, and $d_6 = 1.5D$. Each case shows the periodic nature of the structure. In the case where $N = 1$, we note the emergence of a Fano resonance, resulting from the uniformity of the resonator length. When $N = 3$, this case shows that there are frequencies where the transmission is almost zero (band gaps). In addition, transmission peaks were observed (areas where the transmission curve reached unity). For $N = 5$, corresponding to five waveguide cells, we observed that the number of oscillations increased. The addition of cells modified the resonance characteristics of the structure, resulting in more selective filters with $N = 10$, and the transmission spectrum becomes more complex with a wide band gap. The Fano resonance mode appears in the $N = 1$ case, and its form changes in all other cases, indicating a fundamental characteristic of the structure, in which its position is independent of the number of cells. The insets for cases (c) and (d) provide a more detailed view of the trans-

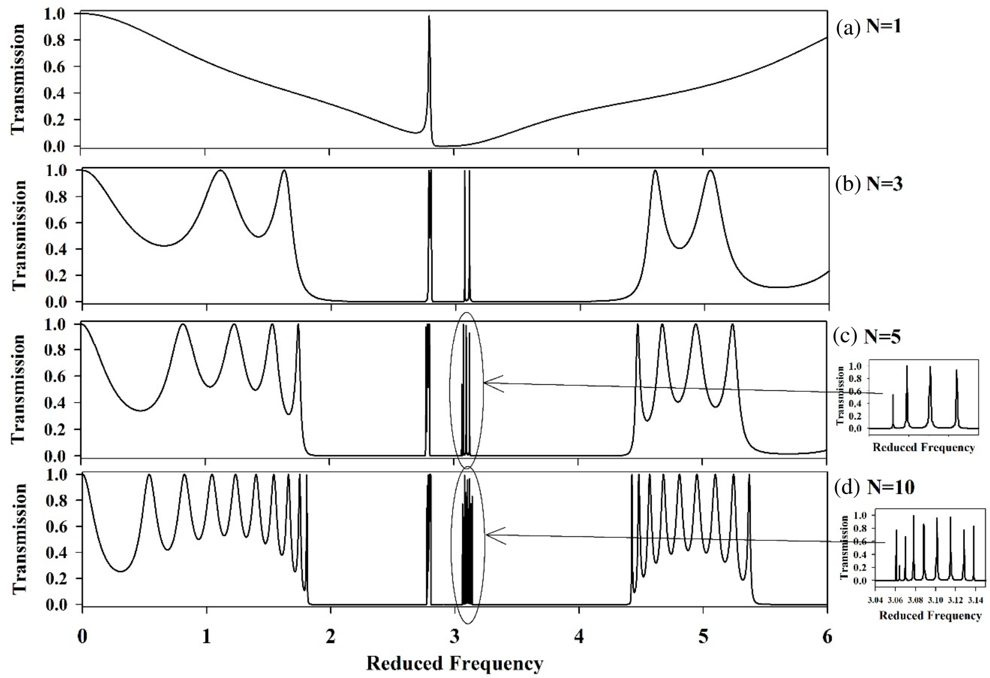

FIGURE 4. Evolution of transmission rate as a function of the reduced frequency for different values of cell numbers N, i.e., (a) $N = 1$, (b) $N = 3$, (c) $N = 5$ and (d) $N = 10$.

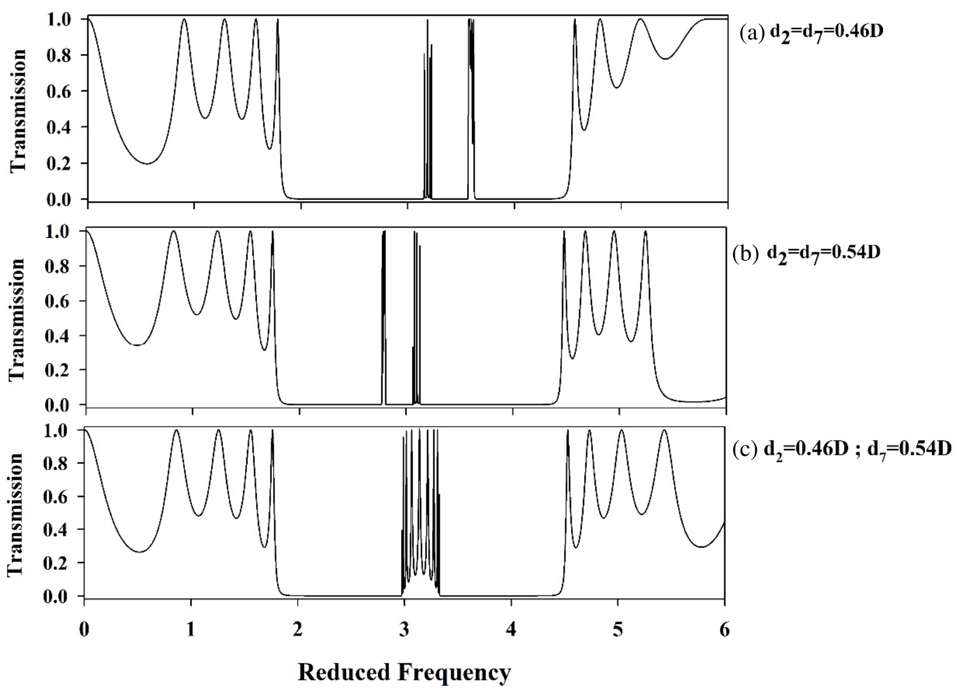

FIGURE 5. Variation of transmission rate as a function of the reduced frequency for a structure containing $N = 5$ cells.

mission peaks at the center of the band gap. As the number of cells increased, the number of peaks increased, as did the number of oscillations in passbands. This could indicate that the system is becoming more selective. We conclude that the interaction between electromagnetic waves and the periodic structure becomes more complex, resulting in selective filters. The presence of band gaps and transmission peaks is crucial for applications, such as frequency filters in telecommunications.

3.4. Influence of Resonator Lengths

Figure 5 shows the variation in the transmission rate as a function of reduced frequency for a finite structure containing $N = 5$ cells. Three different cases of resonator lengths are examined: (a) $d_2 = d_7 = 0.46D$, (b) $d_2 = d_7 = 0.54D$, and (c) $d_2 = 0.46D$, $d_7 = 0.54D$. Figure 5(a) shows the presence of band gaps and transmission peaks. Figure 5(b) and Figure 5(c) suggest that asymmetrical resonator lengths can lead to changes

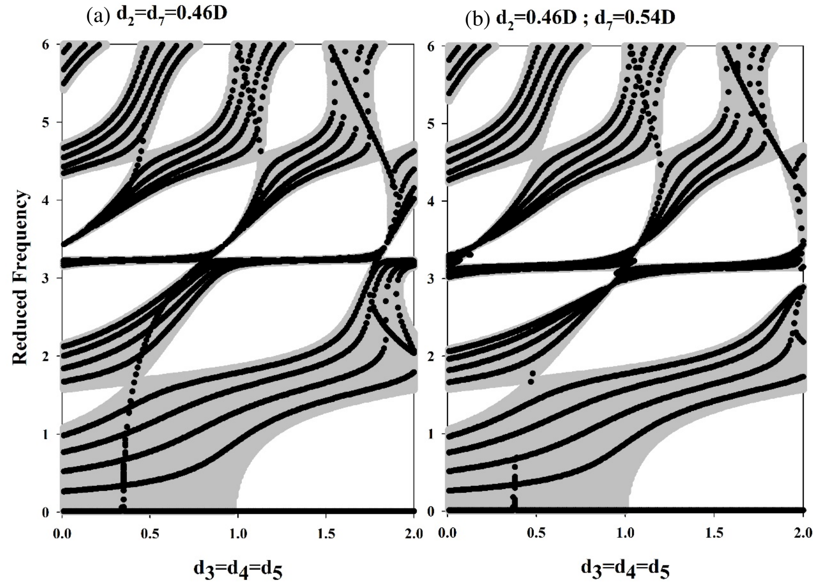

FIGURE 6. Evolution of the reduced frequency as a function of identical lengths $d_3 = d_4 = d_5$ for two cases: (a) $d_2 = d_7 = 0.46D$ and (b) $d_2 = 0.46D$; $d_7 = 0.54D$.

in the position and width of the band gaps. These variations show how the precise geometry of a periodic structure, including the length of the individual elements, can be used to finely control the transmission properties. The differences observed in the transmission profiles for each configuration demonstrate the importance of perfect periodic structure engineering for the development of advanced photonic devices.

3.5. Impact of Waveguide Lengths

Figure 6 shows the evolution of the reduced frequency as a function of the length $d_3 = d_4 = d_5$ for two specific cases of resonator lengths d_2 and d_7. In case (a), the resonators with lengths d_2 and d_7 are equal to $0.46D$. The band structure shows the existence of band gaps and passbands (represented by white areas and black lines, respectively), which show the dependence of the resonant frequencies on the uniform variation of lengths d_3, d_4, and d_5. The white regions indicate the band gaps, whereas the gray regions indicate the passband that can propagate through an infinite perfect periodic structure. In case (b), d_2 is maintained at $0.46D$ while d_7 equals $0.54D$, and we note the change in the frequency band structure. It can be seen that some band gaps become wider, and new passbands appear, which demonstrates the effect of asymmetrical resonator lengths. These cases are the key to understanding how different waveguide geometries affect the transmission properties and can be used to design optical waveguides with specific transmission characteristics.

3.6. Influence of Resonator Length d_2

Figure 7 shows the evolution of the reduced frequency as a function of a resonator length d_2, with $d_7 = 0.46D$ and $d_3 = d_4 = d_5 = 1D$. It can be seen that the variation in length d_2 leads to significant changes in the position and width of the band gaps. This demonstrates the sensitivity of the waveguide

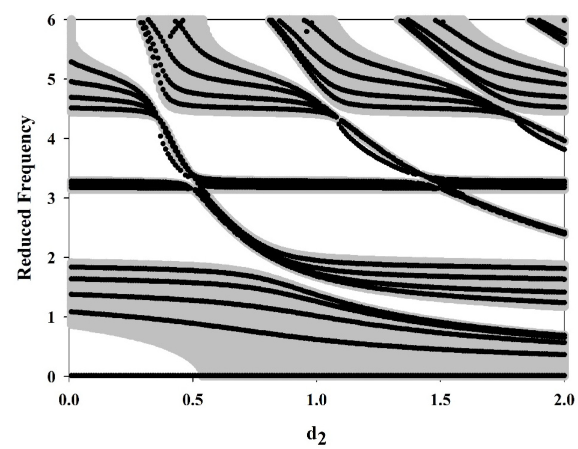

FIGURE 7. Evolution of the reduced frequency as a function of a resonator length d_2 with $d_7 = 0.46D$.

to the physical dimensions of its internal components, underlining the importance of precise design in the development of advanced optical devices. The ability to control the transmission properties in this manner is crucial in many fields, including optical telecommunications.

4. SUMMARY

In this paper, we study the propagation of electromagnetic waves in a 1D perfect periodic structure using the transfer matrix method (TMM), which considers the periodicity of parallel segments and resonators. This system creates passbands separated by band gaps, and electromagnetic waves cannot propagate. Our study suggests the importance of resonator length for guiding, filtering, and investigating the effect of changing the cell number and resonator length on the selective frequency. This study aims to advance the design of devices, such as electromagnetic filters and demultiplexers.

REFERENCES

[1] Du, F., Y.-Q. Lu, and S.-T. Wu, "Electrically tunable liquid-crystal photonic crystal fiber," *Applied Physics Letters*, Vol. 85, No. 12, 2181–2183, 2004.

[2] Mao, Q., K. Xie, L. Hu, Q. Li, W. Zhang, H. Jiang, Z. Hu, and E. Wang, "Light confinement at a dirac point in honeycomb-like lattice photonic crystal," *Optics Communications*, Vol. 384, 11–15, 2017.

[3] Bouzidi, A., D. Bria, A. Akjouj, Y. Pennec, and B. Djafari-Rouhani, "A tiny gas-sensor system based on 1D photonic crystal," *Journal of Physics D: Applied Physics*, Vol. 48, No. 49, 495102, 2015.

[4] Ben-Ali, Y., A. Ghadban, Z. Tahri, K. Ghoumid, and D. Bria, "Accordable filters by defect modes in single and double negative star waveguides grafted dedicated to electromagnetic communications applications," *Journal of Electromagnetic Waves and Applications*, Vol. 34, No. 4, 539–558, 2020.

[5] Cocoletzi, G. H., L. Dobrzynski, B. Djafari-Rouhani, H. Al-Wahsh, and D. Bria, "Electromagnetic wave propagation in quasi-one-dimensional comb-like structures made upof dissipative negative-phase-velocity materials," *Journal of Physics: Condensed Matter*, Vol. 18, No. 15, 3683, 2006.

[6] Yablonovitch, E., "Inhibited spontaneous emission in solid-state physics and electronics," *Physical Review Letters*, Vol. 58, No. 20, 2059, 1987.

[7] John, S., "Strong localization of photons in certain disordered dielectric superlattices," *Physical Review Letters*, Vol. 58, No. 23, 2486, 1987.

[8] Notomi, M., "Manipulating light with strongly modulated photonic crystals," *Reports on Progress in Physics*, Vol. 73, No. 9, 096501, 2010.

[9] Soukoulis, C. M., *Photonic Crystals and Light Localization in the 21st Century*, Springer Science & Business Media, 2012.

[10] Antraoui, I. and A. Khettabi, "Properties of defect modes in a finite periodic structure with branched open resonators," *Materials Today: Proceedings*, Vol. 27, 3132–3138, 2020.

[11] El Kadmiri, I., Y. Ben-Ali, A. Ouariach, A. Khaled, and D. Bria, "Double frequency filtering in one dimensional comb-like phononic structure containing a segment defect," in *Advances in Integrated Design and Production (CPI 2019)*, A. Saka, et al. (eds.), Lecture Notes in Mechanical Engineering, Springer, Cham, 2021.

[12] Ben-Ali, Y., Z. Tahri, F. Falyouni, and D. Bria, "Study about a filter using a resonator defect in a one-dimensional photonic comb containing a left-hand material," in *Proceedings of the 1st International Conference on Electronic Engineering and Renewable Energy (ICEERE 2018)*, B. Hajji, et al. (eds.), Lecture Notes in Electrical Engineering, Vol. 519, Springer, Singapore, 2019.

[13] Vasseur, J. O., B. Djafari-Rouhani, L. Dobrzynski, A. Akjouj, and J. Zemmouri, "Defect modes in one-dimensional comb-like photonic waveguides," *Physical Review B*, Vol. 59, No. 20, 13446, 1999.

[14] Dobrzynski, L., A. Akjouj, B. Djafari-Rouhani, J. O. Vasseur, and J. Zemmouri, "Giant gaps in photonic band structures," *Physical Review B*, Vol. 57, No. 16, R9388, 1998.

[15] Khattab, M. S., T. Touiss, I. E. Kadmiri, F. Z. Elamri, and D. Bria, "Multi-channel electromagnetic filters based on EIT and Fano resonances through parallel segments and asymmetric resonators," *Progress In Electromagnetics Research Letters*, Vol. 115, 105–109, 2024.

[16] Mouadili, A., E. H. E. Boudouti, A. Soltani, A. Talbi, A. Akjouj, and B. Djafari-Rouhani, "Theoretical and experimental evidence of fano-like resonances in simple monomode photonic circuits," *Journal of Applied Physics*, Vol. 113, No. 16, 164101, 2013.

[17] Touiss, T., Y. Errouas, I. E. Kadmiri, and D. Bria, "Electromagnetic filtering with high performance by one dimensional defective comb-like waveguides structure using the transfer matrix," *E3S Web of Conferences*, Vol. 469, 00091, 2023.

[18] Touiss, T., Y. Errouas, A. Ouariach, and D. Bria, "Theoretical design of high-performance guiding and filtering devices using photonic comb-like waveguides with defective resonators," *Journal of Electromagnetic Waves and Applications*, Vol. 38, No. 16, 1779–1795, 2024.

[19] Touiss, T., I. E. Kadmiri, Y. Errouas, and D. Bria, "Electromagnetically induced transparency and Fano resonances in waveguides and U-shaped or cross-shaped resonators," *Progress In Electromagnetics Research Letters*, Vol. 127, 53–63, 2024.

[20] Bria, D., M. B. Assouar, M. Oudich, Y. Pennec, J. Vasseur, and B. Djafari-Rouhani, "Opening of simultaneous photonic and phononic band gap in two-dimensional square lattice periodic structure," *Journal of Applied Physics*, Vol. 109, No. 1, 014507, 2011.